Dust-Grain Charging in Developing Air Plasma

Natalia Yu. Babaeva and Jae Koo Lee, *Senior Member, IEEE*

***Abstract*—The process of a dust-grain charging in developing air plasma with an external source S (cm^{-3} s^{-1}) is studied analytically and numerically in drift-diffusion approximation. It is shown that, when the source is turned on, the steady-state level of electron concentration in the bulk plasma is attained rather quickly (the time being determined by the attachment rate). The time of establishing the ion concentration depends on the source intensity as $S^{-1/2}$. In the steady state, the ratio of ion-to-electron concentrations is proportional to the source intensity as $S^{-1/2}$ and can be very large for low-intensity sources. As a consequence, the process of a dust-grain charging in developing plasma differs significantly for low- and high-intensity sources. At sufficiently high rates of ionization, the grain charge in air is comparable to that in electropositive gases. For low-intensity sources when the ion concentration exceeds that of electron by several orders of magnitude, the grain charge is of the order of several tens of electron charges. The oscillating regime of a dust-grain charging is observed for low-intensity sources.**

***Index Terms*—Air plasma, attachment, dust grain, external source intensity.**

I. Introduction

THE INTEREST in research on dusty plasmas has arisen in recent years in connection with the rapid development of technologies for producing new materials in plasma reactors. (see [1]–[5] and references therein). The dust plasma consists of electrons, ions, neutral gas molecules, and charged dust grains of a micrometer size. Due to the high mobility of electrons, dust grains acquire an equilibrium negative charge matching with the parameters of the surrounding plasma. In a plasma with varying parameters (decaying or developing plasma), this charge is usually a function of time. In the present study, we consider the process of a dust-grain charging in developing atmospheric air plasma with an external source by which the plasma is sustained. We do not specify the nature of the external source. The plasma could be produced either by the electron beam or the radioactive decay products (beam sustained or nuclear induced plasmas). The first problem has been studied in [6] where the external source was associated with the ionization of helium by the electron beam. In [7], the numerical model of the process of a dust-grain charging in nuclear-induced air and xenon plasma has been developed and charges accumulated on the grain surface was compared for plasmas of electropositive and electronegative gases. It has been shown that, at a sufficiently high ionization rate, grains in air were charged by electrons not by ions. For this reason, the dust grain in air acquired an electric charge comparable with that in electropositive gases. Note that in [8], a self-consistent model is presented that takes into account the effect of nonlocal nature of electron energy distribution function on the charging of a dust grain.

Two main processes account for the charge evolution on a dust grain inserted in air plasma in the presence of the external source. The first is connected with the plasma evolution as it would proceed in the absence of a dust grain. This process determines the background concentrations of electrons and ions (which can differ by several orders in magnitude) far from the dust grain. The second process is the dust-grain charging in developing plasma. It is the second process which is the main objective of the present paper. However, our consideration will not be complete and self-consistent if we do not treat the first process properly.

This paper is structured as follows. In Section II, the basic equations are presented which account for processes in developing air plasma coupled with equations for a dust-grain charging. Section III suggests simple analytical approach for consideration the developing air plasma in the absence of a dust grain. The results of simulation of a dust-grain charging are presented in Section IV for weak and strong external sources. In the Appendix, the parameters used for air plasma simulation are indicated.

II. Basic Equations

Following the same approach developed in [9], we consider the process of charging of a spherical conducting dust grain of radius $a = 10\ \mu$m located at the origin of a spherical system of coordinates as shown in Fig. 1. The system of equations for one-dimensional (1-D) spherical coordinates includes the continuity equation for densities of electrons (n_e), positive (n_p), and negative (n_n) ions

$$\frac{\partial n_e}{\partial t} + \frac{1}{r^2}\frac{\partial}{\partial r}(r^2 j_{er}) = S+(\alpha-\eta_2-\eta_3)V_e n_e - \beta_{ei} n_e n_p + \nu_{\det ach} n_n \quad (1)$$

$$\frac{\partial n_p}{\partial t} + \frac{1}{r^2}\frac{\partial}{\partial r}(r^2 j_{\rm pr}) = S + \alpha V_e n_e - \beta_{ei} n_e n_p - \beta_{ii} n_n n_p \quad (2)$$

$$\frac{\partial n_n}{\partial t} + \frac{1}{r^2}\frac{\partial}{\partial r}(r^2 j_{\rm nr}) = (\eta_2+\eta_3)V_e n_e - \beta_{ii} n_p n_n - \nu_{\det ach} n_n \quad (3)$$

where S (cm^{-3}s^{-1}) is the intensity of the external source, r is the magnitude of the radius vector from the origin, α, η_2, and η_3 are ionization, two and three-body attachment coefficients, and β_{ei}, β_{ii} are electron–ion and ion–ion recombination coef-

Manuscript received November 18, 2003; revised December 15, 2003. This work was supported in part by the Korea Ministry of Science and Technology under the Tera-level Nano Devices Project, 21c Frontier R&D Program.

N. Yu. Babaeva is with the Electronics and Electrical Engineering Department, Pohang University of Science and Technology, Pohang 790-784, Korea, on leave from the Institute for High Temperatures, Russian Acadamy of Sciences, Moscow 127412, Russia (e-mail: natalie@postech.ac.kr).

J. K. Lee is with the Electronics and Electrical Engineering Department, Pohang University of Science and Technology, Pohang 790-784, Korea (e-mail: jkl@postech.ac.kr).

Digital Object Identifier 10.1109/TPS.2004.830724

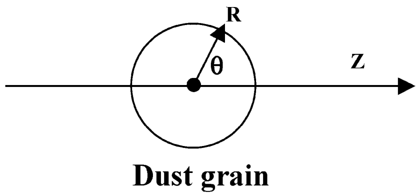

Fig. 1. Dust grain and the coordinate system.

ficient, correspondingly. The right-hand side of the equations represent the sum of contribution of kinetic processes as sources of charged plasma particles. Ionization (detachment) term is included in (1) and (2) as ionization can take place in the electric field produced by charges accumulated on the grain surface (in case of a strong external source). Fluxes of electrons, positive, and negative ions have the following form:

$$\boldsymbol{j}_i = n_i \boldsymbol{V}_i - D_i \nabla n_i, \quad (i = e, p, n) \tag{4}$$

where $\boldsymbol{V}_i$ and D_i denote drift velocities and the diffusion coefficients determined by the magnitude of the electric field. The system of the continuity equations for all the components is closed by the Poisson equation for the potential U

$$\frac{1}{r^2}\frac{\partial}{\partial r}\left(r^2 \frac{\partial U}{\partial r}\right) = -\frac{\rho}{\varepsilon_0} \tag{5}$$

where $\rho = e(n_p - n_n - n_e)$ is the space-charge density. The change of the charge imparted to the particle is given by

$$dQ/dt = e \int_S (\boldsymbol{\Gamma}_p - \boldsymbol{\Gamma}_e - \boldsymbol{\Gamma}_n) \boldsymbol{n}_s \, dS \tag{6}$$

where $\boldsymbol{n}_s$ is the unit vector directed toward the particle surface, dS is the surface element, and e is the absolute value of the electron charge. The fluxes $\boldsymbol{\Gamma}_i (i = e, p, n)$ are calculated as follows:

$$\boldsymbol{\Gamma}_i = s_i n_i \boldsymbol{V}_i - D_i \nabla n_i, (i = e, p, n). \tag{7}$$

The symbol s_i is nonzero only if the drift velocity is directed toward the dust-grain surface ($s_i = 1$, when the product $\boldsymbol{V}_i \boldsymbol{n}_s$ is positive and $s_i = 0$ in the opposite case). It is supposed that the dust grain absorbs every plasma particle hitting its surface. The first term in the right-hand side of (7) represents the so-called drift charging, when the grain is charged by electrons or ions moving in an orderly direction in the electric field. The second term accounts for the diffusion charging. The transport of charged particles to the surface of a dust grain is considered in the drift-diffusion approximation. The electron and ion density at $r = a$ is zero, for the outer boundary the number density of charged particles is determined by the processes in the bulk plasma not disturbed by the presence of a dust grain.

Equations (1)–(7) are solved numerically on the nonuniform mesh, which expands toward the outer boundary. The flux-corrected transport technique which has small numerical diffusion is used for solving the transport equation. The Poisson's equation is solved using the successive over-relaxation method with optimum value of the acceleration parameter ω. Elementary process in air are discussed in the Appendix.

III. Simple Analytical Consideration of the Elementary Processes in the Plasma Bulk

In this section, we consider the processes of establishing steady-state levels of electron and ion concentrations in the bulk plasma (in the absence of a dust grain). These concentrations create the background on which the dust-grain charging occurs. In this case, in the absence of electric field ionization and detachment processes in (1)–(3) can be omitted. For not very intensive external sources ($S < 10^{22} - 10^{24}$ cm^{-3}) the electron–ion recombination term $\beta_{ei} n_e n_i$ is small in comparison with the attachment $\nu_{\text{att}} n_e$. For example, for typical values of $\beta_{ei} = 5 \cdot 10^{-8} - 10^{-7}$ cm^3/s and $\nu_{\text{att}} \sim 10^8$ s^{-1} concentration n_p should reach the level of 10^{15} cm^{-3} for the recombination to be comparable with the attachment. In this case, the external source S would be great enough ($S \cong \beta_{ei} n_p^2 \approx 10^{24}$ cm^{-3} s^{-1}) to support this level of ion concentration. The electron–ion recombination term $\beta_{ei} n_e n_i$ in the right-hand side of (2) can also be omitted as it is small in comparison with the ion–ion recombination. Thus, for the processes in the bulk plasma, we can rewrite (1)–(3) as

$$\frac{\partial n_e}{\partial t} = S - \nu_{\text{att}} n_e \tag{8}$$
$$\frac{\partial n_p}{\partial t} = S - \beta_{ii} n_n n_p \tag{9}$$
$$\frac{\partial n_n}{\partial t} = \nu_{\text{att}} n_e - \beta_{ii} n_n n_p. \tag{10}$$

In the bulk plasma, the electron and ion pairs are produced by the external source. The electrons are lost in attachment process while positive ion are lost primary due to ion–ion rather than electron–ion recombination. The typical time of establishing the stationary electron concentration can be obtained by solving (8) with initial conditions $n_e = n_{e0}(t = 0)$. We have

$$n_e = \frac{S}{\nu_{\text{att}}}(1 - e^{-\nu_{\text{att}} t}) + n_{eo} e^{-\nu_{\text{att}} t}. \tag{11}$$

At small initial values of electron concentration n_{e0} the electron level is stabilized very quickly during $\tau_e \approx 1/\nu_{\text{att}}$.This time does not depend on the external source intensity. For typical values of $\nu_{\text{att}} \approx 8 \cdot 10^7$ s$^{-1} \tau_e$ is of the order of a few tens of nanoseconds. The stationary electron concentration is

$$n_e \approx \frac{S}{\nu_{\text{att}}}. \tag{12}$$

The time evolution of positive ion density can be obtained by solving (9) that can be rewritten with account for quasi-neutrality condition $n_p = n_n + n_e$, when $n_e \ll n_p$. We have

$$\frac{dn_p}{dt} + \beta n_p^2 = S. \tag{13}$$

Equation (13) can readily be integrated to obtain the density of positive ions

$$n_p = \sqrt{\frac{S}{\beta_{ii}}} \frac{C + e^{-2\sqrt{S\beta}t}}{C - e^{-2\sqrt{S\beta}t}} \tag{14}$$

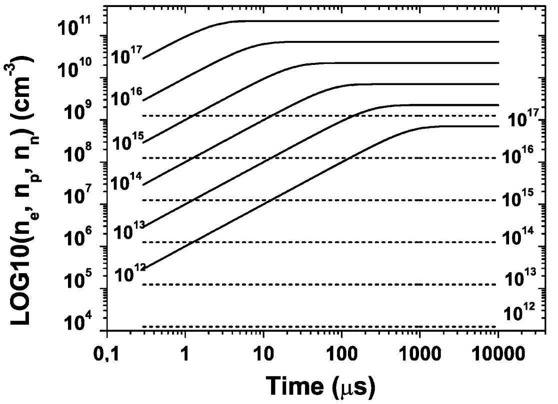

Fig. 2. Evolution of electron (dashed lines) and ion (solid lines) concentration in the bulk plasma for different values of external source intensity. Numbers at the lines denote the source intensity (cm^{-3} s^{-1}). Initial concentrations at $t = 0$ are $n_e = n_p = 10^3$ cm^{-3}. Calculation according to (11) and (14) with $\beta_{ii} = 2 \times 10^{-6}$ cm^3 s^{-1}, $\nu_{\rm att} = 8 \times 10^7$ s^{-1}.

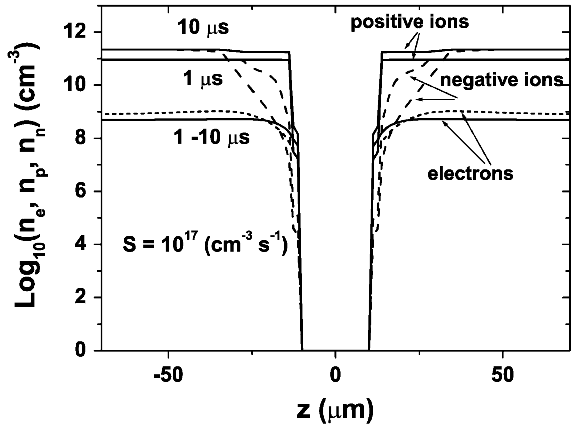

Fig. 3. Strong external source $S = 10^{17}$ cm^{-3} s^{-1}. Distribution of electrons and ions around the dust grain in developing plasma for two time moments 1 μs and 10 μs. The center of the dust grain is located at $z = 0$. The background electron concentration arrives to the steady state very quickly.

where $C = (n_{0p} + \sqrt{S/\beta_{ii}})/(n_{0p} - \sqrt{S/\beta_{ii}})$ and n_{0p} is the initial concentration of positive ions. The stationary concentrations of positive and negative ions are

$$n_p \approx n_n \approx \sqrt{\frac{S}{\beta_{ii}}}. \tag{15}$$

For ions the corresponding time of establishing the steady-state level is $\tau_p \cong 1/\sqrt{S\beta_{ii}}$. This time depends on the external source intensity and can be very large for low intensity sources. The ratio of densities of positive ions to electrons in the plasma bulk can be estimated according to the formula

$$\frac{n_p}{n_e} \approx \frac{\nu_{\rm att}}{\sqrt{S\beta_{ii}}}. \tag{16}$$

In Fig. 2, evolution of electron and ion concentration in the bulk plasma for different values of external sources S calculated according to the formulas (11) and (14) are presented. The steady-state level of ion concentration as well as the time of stabilization depend on the source intensity S. The electron concentrations presented in Fig. 2 by dashed lines are attained very quickly during the first tens of nanoseconds after the source has been turned on. It is seen that ion concentrations grow much slower. The time-dependent levels of ion and electron concentration is an important factor for our further consideration as they determine the background (far from the grain) concentration of plasma particles—ions and electrons.

IV. Results of Simulations and Discussions

We return now to the process of a dust-grain charging in developing plasma maintained by the external source. Self-consistent simulation is performed using (1)–(7). Note that in simulations all the terms in the right-hand side of (1)–(3) are taken into account including ionization, attachment, detachment, electron–ion, and ion–ion recombination. In the Appendix, the parameters used for air plasma simulation are presented.

It is assumed that the dust grain is initially uncharged and placed in the plasma with concentration $n_e \approx n_p = 10^3$ cm^{-3}.

Simultaneously, the external ionization source S is switched on producing the electron–ion pairs. For electronegative gases such as air, depending on the source intensity S, we obtained different levels of charged particles concentrations in the bulk plasma (background levels). The times of establishing the concentrations are different for electrons and ions. After switching on the source, the steady-state electron level is attained rather quickly with typical time determined by the attachment rate. For positive and negative ions, the corresponding time of establishing the steady-state level depends on the source intensity and is very large for low intensity sources. In such a developing plasma, the process of a dust-grain charging exceeds the time of establishing the stationary level of background plasma concentrations. Accumulated charges also depend on the source intensity S. Division on strong and weak external sources is in some sense arbitrary. The source intensity determines the ratio of ion and electron concentration in the bulk plasma (far from the grain). It also defines the intensity of electron diffusion fluxes arriving to the dust-grain surface. Also of importance is the relation between the time moment when the stationary background level of plasma concentration is reached and the moment when (the first) equalization of positive and negative fluxes occurs.

A. Strong External Source

In Fig. 3, concentrations for electron and ions are presented at two different time moments for strong external source $S = 10^{17}$ cm^{-3} s^{-1}. In the 1-D case, we trace the plasma parameters only along the r axis. However, the figures are presented in symmetrical form showing the distribution of plasma parameters along the polar z axis (for polar angles $\theta = 0$ and $\theta = \pi$).

The steady state of electron concentration in the bulk plasma is attained during $\tau_e \approx 1/\nu_{\rm att} \approx 10$ ns and stabilizes at the level of $n_e \approx S/\nu_{\rm att} \approx 10^9$ cm^{-3}. Further redistribution of electron concentration (shown in Fig. 3 by a dotted line) is due to the enhanced electric field caused by charges accumulated on the grain surface. Steady state of ion concentration $n_p \approx n_n \approx \sqrt{S/\beta_{ii}} \approx 10^{11}$ cm^{-3} is reached by the time $\tau_p \cong 1/\sqrt{S\beta_{ii}} \approx 10$ μs. Note, that ion concentration exceeds that of electrons by three orders of magnitude which is in agreement with the simple analytical consideration as indicated in Fig. 2. In Fig. 4, electron, positive, and negative diffu-

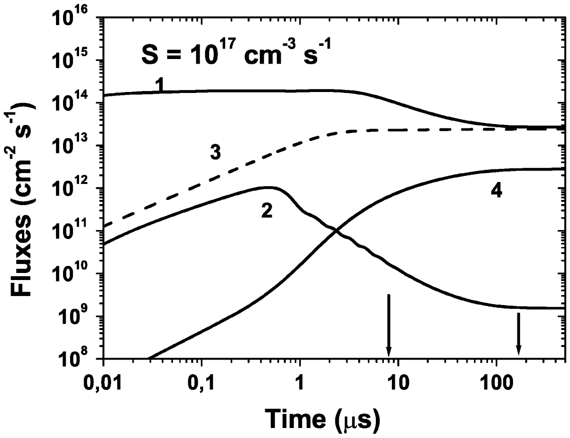

Fig. 4. Strong external source $S = 10^{17}$ cm^{-3} s^{-1}. Fluxes of charged plasma particles collected by the spherical dust grain in developing air plasma. 1) Diffusion flux of electrons. 2) Diffusion flux of negative ions. 3) Diffusion flux of positive ions. 4) Drift flux of positive ions. The first arrow from the left indicates the moment when steady state plasma background concentration is attained. The second arrow shows the moment when ion and electron fluxes equalize and the charge attains its maximal value.

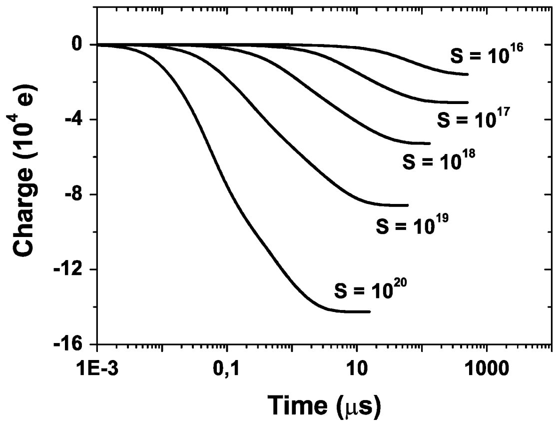

Fig. 5. Time evolution of charge accumulated on the dust grain in developing air plasma for different values of strong external source S.

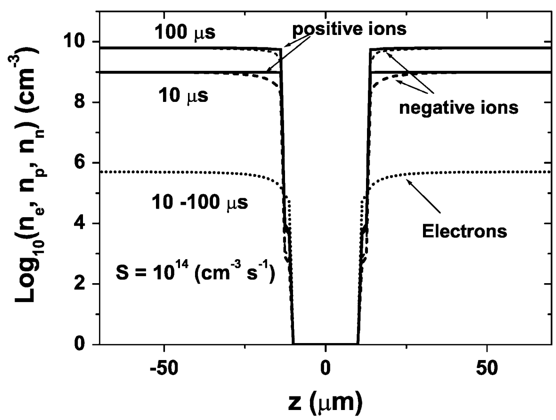

Fig. 6. Weak external source $S = 10^{14}$ cm^{-3} s^{-1}. Distribution of electrons and ions around the dust grain in developing plasma for two time moments 10 and 100 μs. The center of the dust grain is located at $z = 0$.

sive fluxes are shown as a function of time. Electron diffusive flux gives the main contribution to the process of grain charging. This flux determines primarily the charge accumulated on the grain body. It slowly decreases with time as the negative charge on the grain surface increases. On the contrary, the diffusion flux of positive ions grows with time. Drift fluxes of electrons and negative ions are zero as the electric field is directed toward the negatively charged grain surface. Drift flux of positive ions and diffusive flux of negative ions are also small. The first arrow from the left in Fig. 4 indicates the moment when steady state of background concentration is attained (see also the curve for $S = 10^{17}$ cm^{-3}s $^{-1}$ in Fig. 2). Starting from this particular moment, the process of the dust-grain charging occurs at the stationary background plasma conditions. In a steady-state regime, the electron and ion fluxes onto the grain surface are equal to each other. The second arrow in Fig. 4 shows the moment when ion and electron fluxes equalize and the charge attains its maximal stationary value. For strong sources the moment when stationary background concentrations are obtained precedes the moment of fluxes equalization.

Evolution of charges collected by the grain versus time is presented in Fig. 5 for five different values of strong external source. The acquired charges are comparable with those obtained in case of electropositive gases. This result correlates with observation [7] where the process of dust-grain charging in nuclear-induced air plasma was studied numerically. It was stated in [7] that at sufficiently high ionization rates, dust grains are charged by electrons not by ions. For this reason, the dust grain in air can acquire an electric charge comparable with that in electropositive gas.

B. Weak External Source

Weak external source $S = 10^{14}$ cm^{-3} s^{-1}, which we consider in this section, is characterized by much greater difference in electron and ions stationary background concentration as indicated in Fig. 6. In this case, we have $n_e \approx 10^6$ cm^{-3}. This level of background electron concentration, attained during the first tens of nanoseconds, does not change with time during the process of grain charging. Stationary ion concentrations $n_p \approx n_n \approx \sqrt{S/\beta_{ii}} \approx 10^{10}$ cm^{-3} are reached by the time $\tau_p \cong 1/\sqrt{S\beta_{ii}} \approx 100$ μs. In this case, ion background concentration exceeds that of electrons by four orders in magnitude (see also Fig. 2). During the first 10 μs, the electron diffusive flux dominates until the increased diffusion of positive ions exceeds that of electrons. The first arrow from the left in Fig. 7 indicates the moment when ion and electron fluxes equalize for the first time. Charge attains it maximal negative value as shown in Fig. 8. However, by this particular moment, the steady state of background plasma is not reached and the positive flux is still increasing. As a result, the charge on the grain changes the sign. In its turn, it leads to the increase of negative flux (see curve 2 in Fig. 7). The second arrow in Fig. 7 indicates the next moment when positive and negative fluxes become equal and the charge reaches its maximal positive value. The third arrow shows the time when steady state of the plasma background concentration is attained. See also corresponding arrows in Fig. 8, where the charge accumulated on the dust-grain surface is plotted versus time. Note, that for weak sources stationary background concentrations are obtained after the first (the second, etc.) equalization of fluxes occurs. This results in oscillating regime of fluxes and, as a consequence, in oscillating regime of charges collected on

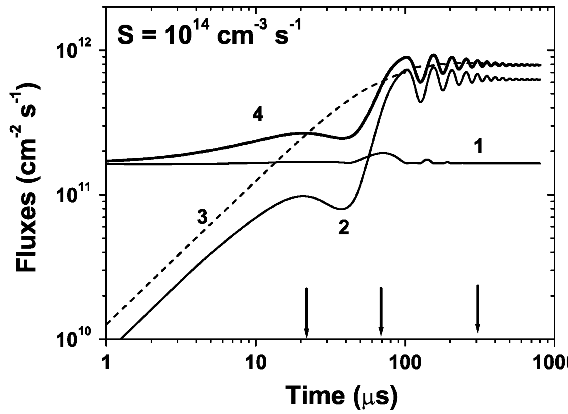

Fig. 7. Weak external source $S = 10^{14}$ cm^{-3} s^{-1}. Fluxes of charged plasma particles collected by the spherical dust grain in developing air plasma. 1) Diffusion flux of electrons. 2) Diffusion flux of negative ions. 3) Diffusion flux of positive ions. 4) Total negative flux of electrons and negative ions. Drift fluxes are negligibly small. The first and the second arrows from the left indicate the moment when ion and electron fluxes equalize for the first and the second time, correspondingly. The third arrow shows the time when the steady state of plasma background concentration is attained. See also the corresponding arrows in Fig. 8.

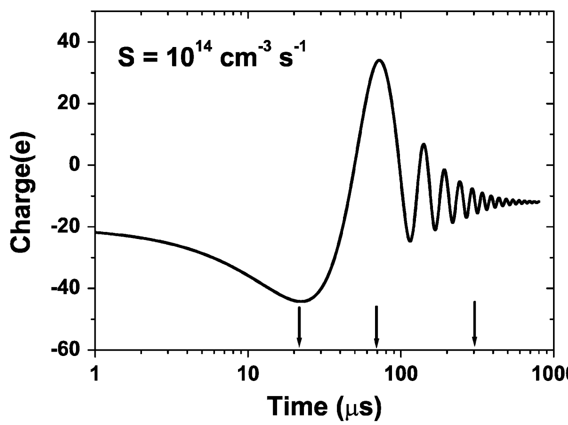

Fig. 8. Time evolution of charge accumulated on the dust grain in developing air plasma for weak external source $S = 10^{14}$ cm^{-3} s^{-1}. Oscillating regime of the dust-grain charge is demonstrated.

the grain surface. The stationary charge in this case is several of electron charges.

V. Conclusion

This paper reports the result of a self-consistent model for a dust-grain charging in electronegative gases with an external source. The evolution of the grain charge is investigated and characteristic time scales on which the grain acquires the charge are established. It is demonstrated that the process of particle charging occurs in a different way for strong and weak external sources and the accumulated charges depend on source intensity. The importance of relation between the time moment when the stationary background level of plasma concentration is reached and the moment when (the first) equalization of positive and negative fluxes occurs is emphasized.

Appendix
Elementary Processes in Air

In this Appendix, the data are presented on the rate constants of elementary processes which are used in our simulations. For the detailed discussion on the appropriate choice of swarm parameters, see [9] and [10] and references therein.

A. Transport Coefficients

The electron swarm data [11] are utilized for the following approximation of drift velocity for electrons:

$$V_e = 3.2{\times}10^5\left(\frac{E}{n}\right)^{0.8} \text{cm/s, E/n is in Td}, 1\text{Td} = 10^{-17}\text{V}{\cdot}\text{cm}^2 \quad (17)$$

and for ions

$$V_{p,n} = C\frac{E}{n}\text{cm/s, E/n is in Td} \quad (18)$$

, where coefficient $C = 5.5 \cdot 10^2$ is for positive ions and $C = 8.25 \cdot 10^2$ stands for negative ions. The diffusion coefficients for electrons for atmospheric pressure air is approximated by the following equation at a gas temperature of 293 K:

$$D_e = 7 \times 10^2 + 8 \times \left(\frac{E}{n}\right)^{0.8} \quad (19)$$

(cm^2/s, E/n is in Td).

B. Diffusion for Positive and Negative Ions

The diffusion coefficient for positive $(i = p)$ and negative $(i = n)$ ions is defined using Einstein relation

$$\frac{D_i}{\mu_i} = k_B\frac{T_i}{e} \quad (20)$$

where T_i is the ion temperature which depends on E/n. T_i can be evaluated according to Wannier formula (see [12])

$$T_i = T_g + \frac{1}{3}(m_i + m)V_i^2. \quad (21)$$

Here, m_i and m are masses of the ion and the molecule, V_i is the drift velocity of the ion for the given E/n, and T_g is the gas temperature.

C. Ionization

The value of electron-impact ionization coefficient α/n is approximated by

$$\frac{\alpha}{n} = \left(1 + \frac{6 \cdot 10^6}{(E/n)^3}\right) \cdot 5 \cdot 10^{-16}\exp\left(-\frac{1010}{E/n}\right) \quad (22)$$

(cm^2, E/n is in Td).

D. Recombination

At pressures about 1 atmosphere, the ion–ion recombination coefficient weakly depends on pressure. Its value in air is [13]

$$\beta_{ii} = 2 \times 10^{-6}\left(\frac{300}{T_i}\right)^{1.5} \quad (23)$$

(cm^3 s^{-1}), where T_i can be evaluated according to (21). For the electron and positive ion recombination in air, the value $\beta_{\text{ei}} =$

5×10^{-8} cm^3/s is used typical for simple ions (N_2^+, O_2^+, and NO^+).

E. Electron Attachment

Two types of attachment are taken into account—three- and two-body attachment. In rather weak electric fields, the process of three-body attachment is essential. In the present paper, for three-body attachment coefficient η_3/n^2 the following approximation is used as the best fit to the experimental data in the form of explicit dependence on E/n [12]

$$\frac{\eta_3}{n^2} = 1.6 \times 10^{-37}(E/n)^{-1.1} \tag{24}$$

(cm^5, E/n is in Td).

Expression (24) overestimates the attachment coefficient for low and zero electric fields. In [15], an approximation of experimental data gives the following expressions for corresponding attachment rate coefficient:

$$K_{\text{att3}} = 1.4 \times 10^{-29} \times \frac{300}{T_e} \times \exp\left(-\frac{600}{T_g}\right) \times \exp\left(\frac{700 \times (T_e - T_g)}{T_e \times T_g}\right) \tag{25}$$

(cm^6 s^{-1}). Expression (25) is used to estimate the value of the attachment rate $\nu_{\text{att3}} \sim 8 \cdot 10^7$ s^{-1} in zero electric fields (when $T_e \approx T_g$) that is considered to be the upper limit for it.

For rather high values of electric field the reaction of dissociative attachment must be taken into account. The two-body attachment coefficient in air can be approximated as

$$\frac{\eta_2}{n} = 4.3 \cdot 10^{-19} \exp(-1.05 \cdot |5.3 - \log 10(E/n)|^3) \tag{26}$$

(cm^2). The sum of two- and three-body attachment rates (at gas pressure $\mathrm{P} = 760$ torr) is related with two- and three-body attachment coefficients by the expression $\nu_{\text{att}} = (\eta_2 + \eta_3)V_e$. For rather weak electric fields considered in the paper, attachment mainly occurs due to three body collisions.

F. Detachment

In order to determine the effective rate at which electrons are removed from negative ions, it is necessary to know the ion composition of the plasma. In the present paper, the detachment rate coefficient

$$K_{\det\text{ach}} = 2 \times 10^{-10} \exp\left(-\frac{6030}{T_i}\right) \tag{27}$$

(cm^3 s^{-1}) is used which corresponds to the abundance of O_2^- ions [12] with the effective ion temperature T_i calculated according to (21).

Acknowledgment

The authors gratefully acknowledge helpful discussions with Prof. G. V. Naidis and Prof. M. S. Benilov.

References

[1] S. J. Choi and M. J. Kushner, "A particle-in-cell simulation of dust charging and shielding in low pressure glow discharge," *IEEE Trans. Plasma Sci.*, vol. 22, pp. 138–150, Apr. 1994.

[2] V. E. Fortov, A. P. Nefedov, V. I. Molotkov, M. Y. Poustylnik, and V. M. Torchinsky, "Dependence of the dust-particle charge on its size in a glow-discharge plasma," *Phys. Rev. Lett.*, vol. 87, Nov. 2001.

[3] L. Boufendi and A. Bouchoule, "Industrial developments of scientific insights in dusty plasmas," *Plasma Sources Sci. Technol.*, vol. 11, pp. A211–A218, Aug. 2002.

[4] P. K. Shukla and A. A. Mamun, *Introduction to Dusty Plasma Physics*. Bristol, U.K.: IOP, 2002.

[5] M. S. Hur, H. J. Lee, and J. K. Lee, "Ion-beam-driven instabilities in bounded dusty plasmas," *IEEE Trans. Plasma Sci.*, vol. 27, pp. 1449–1453, Oct. 1999.

[6] V. V. Ivanov, T. V. Rakhimova, A. O. Serov, N. V. Suetin, and A. F. Pal, "Effect of a dust component on the rates of elementary processes in low-temperature plasmas," *J. Exp. Theor. Phys. (JETP)*, vol. 88, pp. 1105–1113, June 1999.

[7] A. F. Pal, A. N. Starostin, and A. V. Filippov, "Charging of dust grain in a nuclear-induced plasma at high pressures," *Plasma Phys. Rep.*, vol. 27, pp. 143–152, Feb. 2001.

[8] A. V. Filippov, N. A. Dyatko, A. F. Pal, and A. N. Starostin, "Development of a self-consistent model of dust grain charging at elevated pressures using the method of moments," *Plasma Phys. Rep.*, vol. 29, no. 3, pp. 190–202, Mar. 2003.

[9] N. Yu. Babaeva, J. K. Lee, and H. C. Kim, "Non-stationary charging of a dust grain in decaying streamer-channel plasma," *Plasma Sources Sci. Technol.*, to be published.

[10] N. Yu. Babaeva and G. V. Naidis, "Dynamics of positive and negative streamers in air in weak uniform electric fields," *IEEE Trans. Plasma Sci.*, vol. 25, pp. 375–379, Apr. 1997.

[11] J. W. Gallagher, E. C. Beaty, J. Dutton, and L. C. Pitchford, "An annotated compilation and appraisal of electron swarm data in electronegative gases," *J. Phys. Chem. Ref. Data*, vol. 12, pp. 109–152, 1983.

[12] A. Kh. Mnatsakanyan and G. V. Naidis, "Charged particle production and loss processes in nitrogen-oxygen plasmas," in *Reviews of Plasma Chemistry*, B. M. Smirnov, Ed. New York: Consultants Bureau, 1991, pp. 259–292.

[13] B. M. Smirnov, *Negative Ions*. New York: McGraw-Hill, 1982.

[14] G. V. Naidis, "Simulation of streamer-to-spark transition in short nonuniform air gaps," *J. Phys. D, Appl. Phys.*, vol. 32, pp. 2649–2654, Oct. 1999.

[15] I. A. Kossyi, A. Yu. Kostinsky, A. A. Matveyev, and V. P. Silakov, "Kinetic scheme of the nonequilibrium discharge in nitrogen-oxygen mixtures," *Plasma Sources Sci. Technol.*, vol. 1, pp. 207–220, 1992.

Natalia Yu. Babaeva was born in Klin, Moscow Region, U.S.S.R. (now Russia). She received the M.S. degree (with honors) in physics and engineering from the Moscow Institute for Physics and Technology, in 1982 and the Ph.D. degree in plasma physics and chemistry from the Institute for High Temperatures, Russian Academy of Sciences, Moscow, in 1993.

Since November 2001, she has been an Assistant Professor with Pohang University of Science of Technology, Pohang, Korea, on leave from the Institute for High Temperatures. Her research interests include physics of gas discharges, numerical modeling of low-temperature plasmas, and RF discharges.

Jae Koo Lee (M'83–SM'02) received the Ph.D. degree from the University of California, Berkeley, in 1979.

From 1979 to 1989, he was a Senior (later a Staff) Scientist on Tokamak theory with General Atomics, San Diego, CA. He is currently a Professor in the Department of Electronic and Electrical Engineering, Pohang University of Science and Technology, Pohang, Korea. He is currently on the Editorial Board of *Plasma Source and Science and Technology*. His research interests include the theory and simulation of low-temperature basic/processing plasmas, fusion plasmas, and free-electron lasers.

Prof. Lee is the past Chair of Division of Plasma Physics of Korean Physical Society.